Report

Cofilin Tunes the Nucleotide State of Actin Filaments and Severs at Bare and Decorated Segment Boundaries

Cristian Suarez,[1] Jérémy Roland,[1]
Rajaa Boujemaa-Paterski,[1] Hyeran Kang,[2]
Brannon R. McCullough,[2] Anne-Cécile Reymann,[1]
Christophe Guérin,[1] Jean-Louis Martiel,[1]
Enrique M. De La Cruz,[2,*] and Laurent Blanchoin[1,*]
[1]Laboratoire de Physiologie Cellulaire et Végétale, Institut de Recherches en Sciences et Technologies pour le Vivant, CEA/CNRS/INRA/UJF, F-38054 Grenoble, France
[2]Department of Molecular Biophysics and Biochemistry, Yale University, New Haven, CT 06520, USA

Summary

Actin-based motility demands the spatial and temporal coordination of numerous regulatory actin-binding proteins (ABPs) [1], many of which bind with affinities that depend on the nucleotide state of actin filament. Cofilin, one of three ABPs that precisely choreograph actin assembly and organization into comet tails that drive motility in vitro [2], binds and stochastically severs aged ADP actin filament segments of de novo growing actin filaments [3]. Deficiencies in methodologies to track in real time the nucleotide state of actin filaments, as well as cofilin severing, limit the molecular understanding of coupling between actin filament chemical and mechanical states and severing. We engineered a fluorescently labeled cofilin that retains actin filament binding and severing activities. Because cofilin binding depends strongly on the actin-bound nucleotide, direct visualization of fluorescent cofilin binding serves as a marker of the actin filament nucleotide state during assembly. Bound cofilin allosterically accelerates P_i release from unoccupied filament subunits, which shortens the filament ATP/ADP-P_i cap length by nearly an order of magnitude. Real-time visualization of filament severing indicates that fragmentation scales with and occurs preferentially at boundaries between bare and cofilin-decorated filament segments, thereby controlling the overall filament length, depending on cofilin binding density.

Results and Discussion

Direct Visualization of ADF/Cofilin Binding to Growing Actin Filaments

To follow in real time ADF/cofilin binding to actin filaments, we engineered a yeast ADF/cofilin mutant that could be specifically labeled with a fluorescent probe. Yeast ADF/cofilin contains a single cysteine residue that is buried in the protein structure, so we substituted D34, a solvent-exposed amino acid residue positioned outside of the actin-binding site [4], to cysteine (Figure 1A) and labeled with Alexa-488 maleimide (Figure 1B). Labeled D34C ADF/cofilin retains strong actin filament binding (see Figure S1A available online), severing (discussed forthcoming), and acceleration of spontaneous actin

assembly activities (Figure S1B). Given the minimal perturbations of substitution and labeling, Alexa-488-labeled ADF/cofilin is a reliable tool to investigate the dynamic interaction with elongating actin filaments.

We followed in real time using total internal reflection fluorescence microscopy (TIRFm) the interaction of ADF/cofilin with actin filaments as they spontaneously assembled from Alexa 568-labeled ATP-actin monomers (Figures 1C and 1E). Measurements were done in the presence of profilin to foster nucleotide exchange from actin monomers, thereby maintaining an ATP-actin monomer pool [5] and limiting ADF/cofilin binding to monomers in solution. The cumulative fluorescence of labeled actin in the evanescent field (proportional to polymer mass) increases linearly over time (Figure 1E), yielding a filament elongation rate of ≈ 5 subunits s^{-1} (Figure 1E) in the absence of ADF/cofilin, consistent with previous determinations [6].

Using two-color TIRFm, we simultaneously monitored in real time actin filament assembly and ADF/cofilin binding (Figures 1D and 1F and Movie S1). The density of bound ADF/cofilin scales with the increase in total polymer (Figure 1F). Remarkably, we detect only minor ADF/cofilin fluorescence before 170 s of actin assembly at the TIRFm resolution scale (Figure 1D), demonstrating that ADF/cofilin binding is delayed relative to actin polymerization, presumably because of the nucleotide state of filament subunits [5].

Bound ADF/Cofilin Dissociates Slowly from Actin Filaments

The lifetime and dissociation kinetics of bound ADF/cofilin were evaluated by fluorescence recovery after photobleaching (FRAP). A defined segment of an Alexa-488-ADF/cofilin-decorated filament was photobleached with an intense laser beam (Figure 2A, white box). Surprisingly, minimal fluorescence recovery associated with alexa-488-ADF/cofilin occurs within 500 s, indicating that the rate constant for yeast ADF/cofilin dissociation from filaments is very slow and negligible over the time courses of experimental visualization (Figure 2B and Movie S2). Locally bleached actin filaments elongate and bind Alexa-488-ADF/cofilin, thereby confirming that neither actin nor ADF/cofilin are limiting (Figure 2A, green box, and Figure 2C) and that the lack of ADF/cofilin recovery after photobleaching (Figures 2A and 2B) reflects slow ADF/cofilin dissociation.

To ensure that slow yeast ADF/cofilin dissociation is not a consequence of labeling or photobleaching procedures, we competed bound unlabeled ADF/cofilin with Alexa-labeled ADF/cofilin (Figure 2E and Movie S2). Undetectable levels of Alexa-ADF/cofilin incorporate into actin filaments decorated with unlabeled ADF/cofilin filaments within 800 s (Figure 2E), thereby confirming that slow ADF/cofilin dissociation is an intrinsic biochemical property of yeast ADF/cofilin that contributes to a high overall binding affinity [7]. Note that Alexa-488-ADF/cofilin binds rapidly to bare actin filaments (Figure 2D and Movie S2).

ADF/Cofilin Shortens the ATP/ADP-P_i Cap Length of Actin Filaments by Allosterically Accelerating P_i Release

ADF/cofilin binds 40-fold more strongly to ADP-actin filament subunits than to ATP or ADP-P_i subunits and weakens

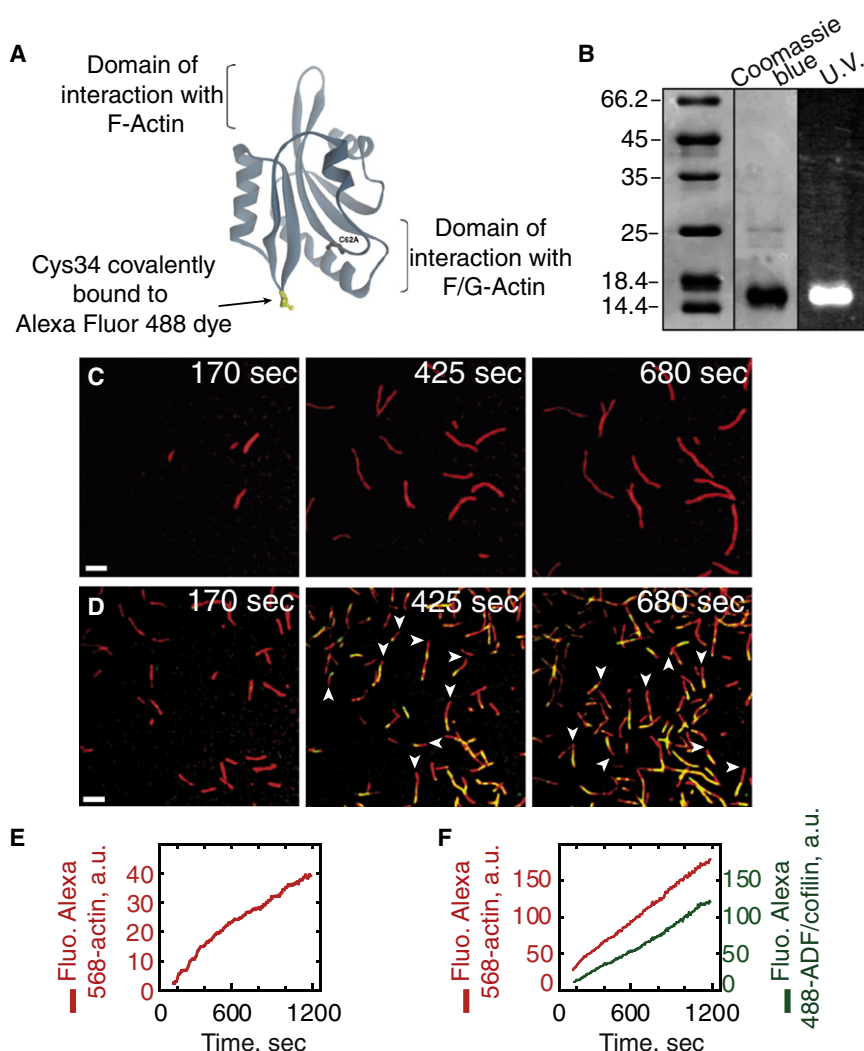*Correspondence: enrique.delacruz@yale.edu (E.M.D.L.C.), laurent.blanchoin@cea.fr (L.B.)

Figure 1. Direct Visualization of ADF/Cofilin Binding on Elongating Actin Filaments by Evanescent Wave Microscopy

(A) Structure of *S. cerevisiae* cofilin (Protein Data Bank ID code COF1); its only cysteine (C62) radical is buried in the wild-type protein structure. We designed a mutant D34C-cofilin with a solvent-exposed cysteine that is available for labeling by Alexa dyes.

(B) A 15% SDS-PAGE gel of purified Alexa-488-labeled D34C-cofilin revealed both by Coomassie blue staining and ultraviolet illumination.

(C–F) Montage of time-lapse total internal reflection fluorescence microscopy (TIRFm) images showing the polymerization of 0.8 μM Alexa-568-labeled actin with 2.4 μM profilin in the absence (C, E) or presence (D, F) of 0.92 μM Alexa-488-cofilin. Alexa-568-actin filaments were colored in red, Alexa-488-ADF/cofilin in green, and the decorated portions of filaments in yellow in the merged images (D). White arrowheads indicate the fast-growing barbed ends of filaments. (E) shows the increase of the integrated intensity fluorescence over time along actin filaments (red curve) in (C), whereas (F) shows that of actin filaments (red curve) and bound Alexa-488-cofilin (green curve) in (D). Scale bars represent 5 μm.

saturating concentration of ADF/cofilin and in the presence of 0.8 μM actin (Figure 3B). Higher ADF/cofilin concentrations do not shorten the cap length (Figure 3B), which remains stationary over time, whereas the aged zone of the filament is decorated with ADF/cofilin (Figure S1C).

A kinetic model in which the nucleotide-linked equations of actin filament nucleation, elongation, random ATP hydrolysis, P_i release, and ADF/cofilin binding are explicitly accounted for was used to fit the experimental cap length data (Figures 3B and 3C and Supplemental Experimental Procedures). The ADF/cofilin concentration dependence of the cap length is well described by a model in which bound ADF/cofilin increases P_i release from ADP-P_i subunits by an order of magnitude from 0.0019 s^{-1} to 0.013 s^{-1} (Figure 3B; [5]). The fit to the data, however, is significantly improved if acceleration of P_i release is propagated allosterically from ADF/cofilin-occupied sites to ≥10 vacant subunits along the filament (i.e., nonnearest neighbor effects), as predicted from long-range effects on filament subunit torsional dynamics [13].

The actin filament ATP/ADP-P_i cap size (at a given actin concentration) is determined by the maximum P_i release rate constant, even though it is accelerated allosterically by ADF/cofilin binding. This behavior predicts that the cap length increases linearly with actin concentration and also with inclusion of P_i in the medium, as is observed (Figures 3C and 3D). Similarly, if filament barbed end elongation is stopped with capping protein, the ATP/ADP-P_i cap disappears and ADF/cofilin decorates the entire filament (Figure S1D). Taken together, these results demonstrate that the ATP/ADP-P_i cap length reflects a tight balance between filament elongation, random ATP hydrolysis, ADF/cofilin binding, and allosteric acceleration of P_i release from vacant filament subunits.

P_i binding by accelerating release from ADP-P_i subunits through thermodynamic and kinetic linkage [5]. Labeled ADF/cofilin therefore serves as an effective marker to directly probe the nucleotide composition of individual actin filaments. TIRFm reveals that ADF/cofilin does not decorate filament barbed end segments, even at high ADF/cofilin concentration (Figure 3A, middle and bottom, and Movie S3), which we interpret as weak binding to ATP/ADP-P_i cap at filament barbed ends (Figure 3A). We note that the filament is comprised predominantly of ADP-P_i subunits at these actin concentrations and in the absence of ADF/cofilin (Figure 3A, top; [8, 9]), to which ADF/cofilin binds very weakly [5, 10]. ADF/cofilin must therefore accelerate P_i release from filaments, as reported for assays done with bulk filament populations [5], to decorate with such high efficiency (Figure 3A, middle and bottom). In addition, observation of multiple ADF/cofilin clusters along individual actin filaments favors a random ATP hydrolysis mechanism for filament subunits over a vectorial mechanism (Movie S1 and Movie S3).

Because the ATP/ADP-P_i cap size can be limited both by slow ADF/cofilin binding [11, 12] and/or by the rate of P_i release, we investigated the variation in cap length as a function of ADF/cofilin and actin monomer concentrations. Statistical analysis reveals that the mean cap length depends on the ADF/cofilin concentration, reaching a minimum of 1.6 μm at
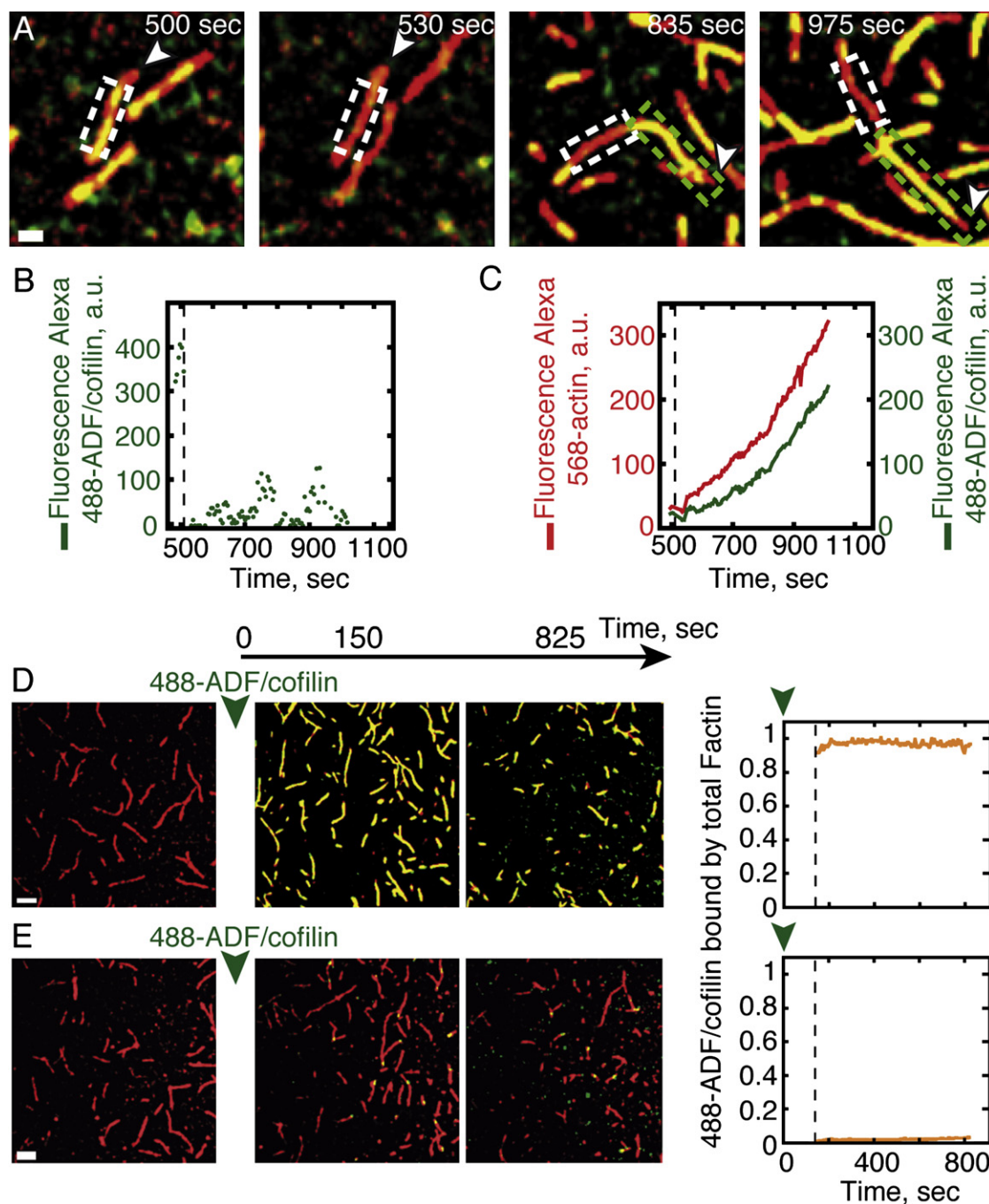
Figure 2. The ADF/Cofilin Turnover on Actin Filaments Is Limited by Its Slow Off-Rate Constant

The polymerization of 0.8 μM Alexa-568-actin monomers in the presence of 2.4 μM profilin and 1.8 μM Alexa-488-ADF/cofilin (A) or 2 μM Alexa-488-ADF/cofilin (D) was followed by TIRFm. Fluorescence signals were colored as in Figure 1.

(A–C) FRAP assays were performed on Alexa-488-ADF/cofilin in interaction with growing actin filaments. After 500 s of actin polymerization, Alexa-488-ADF/cofilin fluorescence was bleached (dashed white box) and the fluorescence recovery was followed over a period of an additional 500 s of actin assembly (A). The actin filament was still elongating outside of the bleached box by its fast-growing barbed end (white arrowhead) and was decorated by Alexa-488-ADF/cofilin (green box, A). After photobleaching, the integrated Alexa-488-ADF/cofilin fluorescence over time in the bleached area (dashed white box) remained negligible compared to its initial value (B); however, in (C), the integrated fluorescence intensities of both Alexa-568-actin filaments and Alexa-488-ADF/cofilin outside the bleached area still increase over time (green box).

(D) Pulse-chase experiments. We added 2 μM Alexa-488-ADF/cofilin to 0.8 μM Alexa-568-actin saturated with 2.4 μM profilin after 3 min of polymerization. (E) Same as in (D), but actin polymerization occurred in the presence of 2 μM unlabeled ADF/cofilin before addition of Alexa-488-ADF/cofilin. Time zero corresponds to the addition of 2 μM Alexa-488-ADF/cofilin. The rightmost graphs show that the integrated fluorescence intensity of Alexa-488-ADF/cofilin bound along the bare actin filament (D) and along the actin filament preincubated with unlabeled-ADF/cofilin (E). Scale bars represent 2 μm in (A) and 5 μm in (D).
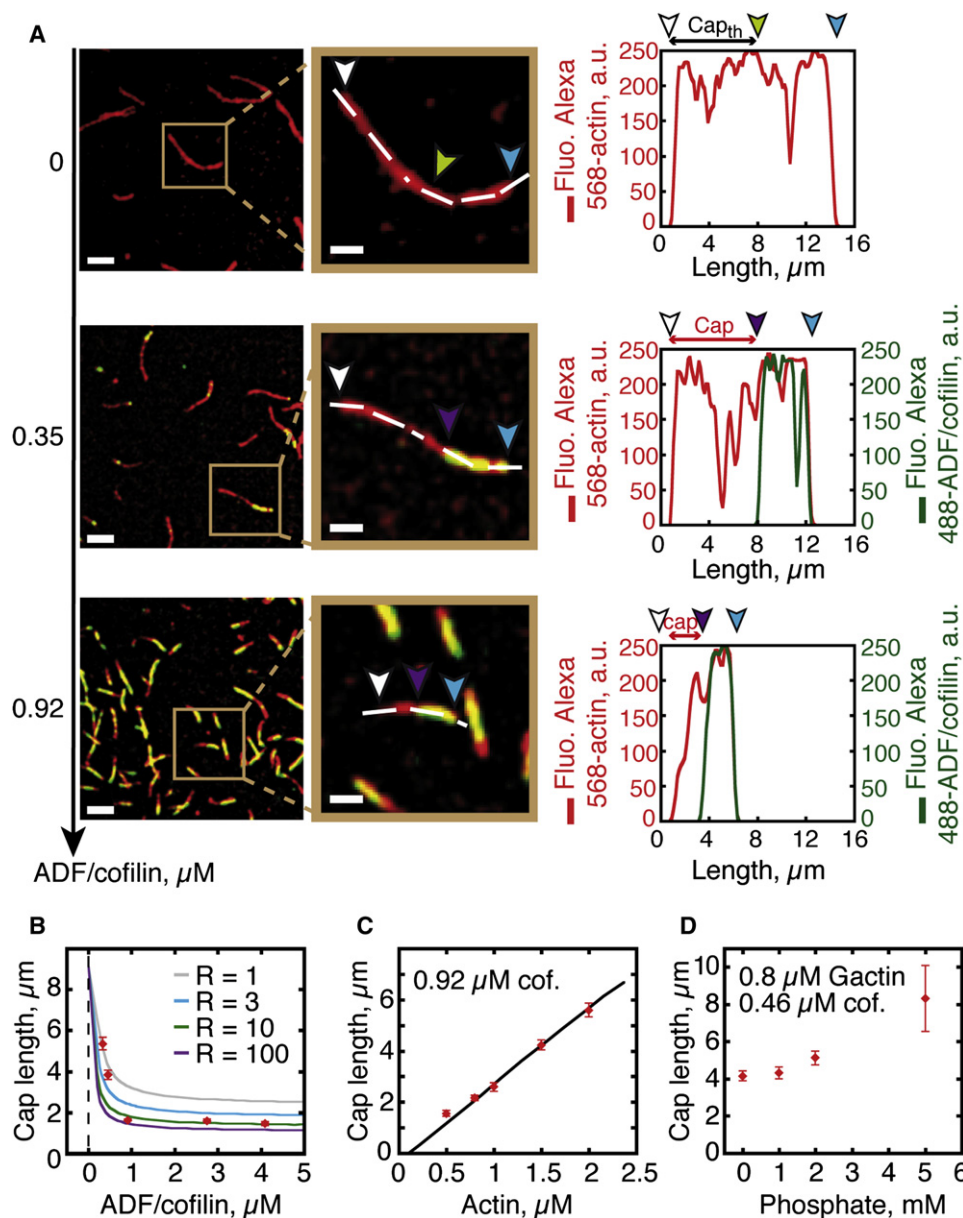
Figure 3. Tight Coupling between Binding and Effect on Nucleotide State of Actin Filaments Modulates ADF/Cofilin-Actin Interaction

(A) 0.8 μM Alexa-568-actin monomers were polymerized in the presence of 2.4 μM profilin and ADF/cofilin, as indicated. TIRFm images were taken at 800 s. Fluorescence signals were colored as in Figure 1. The images in the middle column are zooms of the boxed areas in the left column. Arrowheads indicate pointed ends (blue), barbed ends (white), and the ATP/ADP-P_i cap length (white to purple). In the absence of ADF/cofilin, the theoretical position of the interface between ADP-P_i and ADP zones (green) was determined according to the slow phosphate release, whose half-life time is ~6 min [5]. In the presence of ADF/cofilin, the cap length is determined by the absence of fluorescence in the green channel (middle and bottom). Graphs in the rightmost column quantified the fluorescence intensity of Alexa-568-actin and Alexa-488-ADF/cofilin along actin filament length, marked by a dashed line. Scale bars represent 5 μm and 2 μm, respectively, for the left and middle columns.

(B) Allosteric effect of ADF/cofilin on ATP/ADP-P_i cap length. Experimental data (dots) were fitted by a kinetic model (lines, see Supplemental Experimental Procedures) as a function of Alexa-488-ADF/cofilin concentrations. We varied in the model the R value, which represents how P_i release is propagated allosterically from ADF/cofilin-occupied sites to 1 (gray), 3 (blue), 10 (green), or 100 (purple) vacant subunits along the filament.

(C) The experimental ATP/ADP-P_i cap (dots) increases linearly with the concentration of actin monomers in solution, as predicted by the model (line).

(D) Variation of the ATP/ADP-P_i cap length in the presence of an increasing concentration of inorganic phosphate in the medium.

Error bars in (B)–(D) represent the standard deviation of the cap length measured for each condition.

Actin Filament Severing Occurs at Low ADF/Cofilin Binding Densities and Preferentially at Boundaries of Bare and ADF/Cofilin-Decorated Segments
Direct, real-time visualization of ADF/cofilin binding to actin filaments also permits evaluation of the sites of severing and identification of how they correlate with filament occupancy. Of

particular importance is identifying the site or sites of preferential filament fragmentation. That is, whether it occurs preferentially at junctions of bare and decorated regions [14] or internally within homogenous (bare or ADF/cofilin-decorated) segments.

ADF/cofilin binding alters the average structure [15, 16] and dynamics [7, 13, 17, 18] of actin filaments such that they are
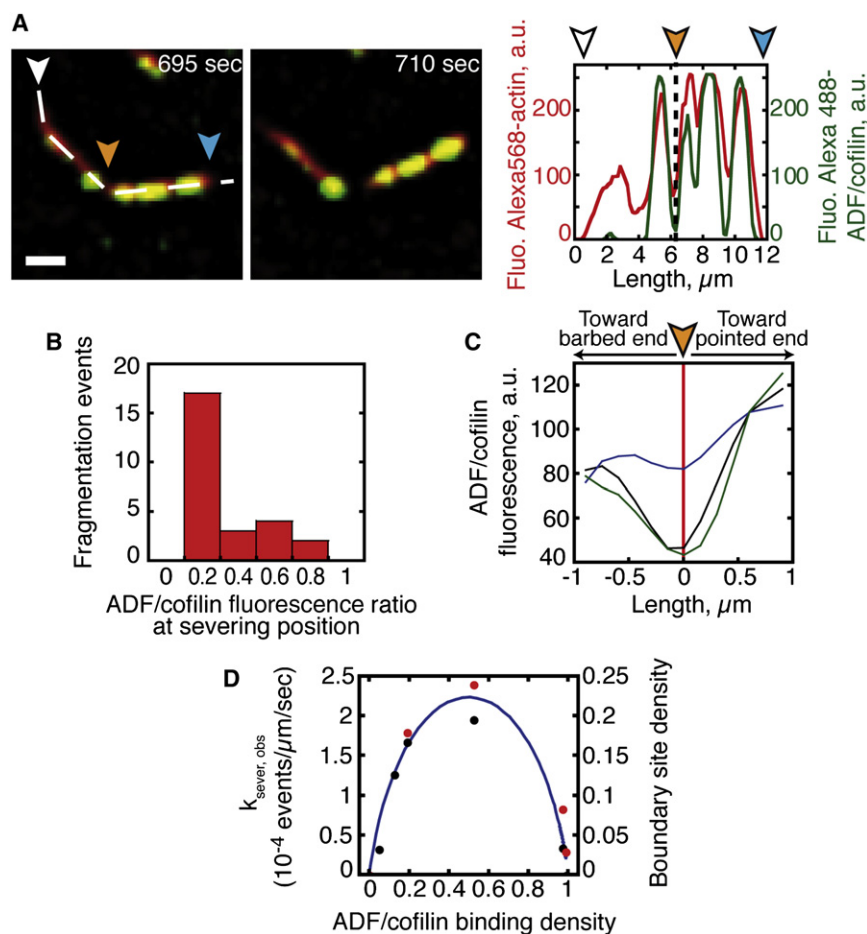
Figure 4. ADF/Cofilin Severing Occurs between Regions of Bare and ADF/Cofilin-Decorated Actin Filaments

(A) The polymerization of 0.5 μM Alexa-568-actin monomers in the presence of 1.5 μM profilin and 0.3 μM Alexa-488-cofilin was followed by TIRFm. The distribution of Alexa-568-actin and Alexa-488-cofilin along the filament was quantified using line scans of their respective fluorescence (dashed line). Fluorescence signals were colored as in Figure 1. The arrowheads (orange) indicate the position of the actin filament's severing site, barbed end (white), and pointed end (blue). Scale bars represent 2 μm.

(B) The histogram quantified the frequency of fragmentation events as a function of the ratio of Alexa-488-ADF/cofilin over actin filament.

(C) Statistics of the Alexa-488-ADF/cofilin fluorescence ratio, calculated as in (B), along fragmented filaments, which were centered on their fragmentation site (red line). The curves give the average of the fluorescence ratio (n = 28) for 0.5 μM (black), 0.9 μM (blue), and 2.8 μM Alexa-488-ADF/cofilin (green curve).

(D) ADF/cofilin severing activity (red dots for labeled ADF/cofilin and black dots for unlabeled ADF/cofilin) scales with the density of boundaries between bare and ADF/cofilin-decorated filament segments (solid line). The ADF/cofilin binding density (cofilins bound per actin subunit) and the fractional site density of boundaries between bare and ADF/cofilin-decorated segments (solid line) were calculated from the Alexa-488-labeled ADF/cofilin or unlabeled ADF/cofilin binding parameters, determined in equilibrium binding measurements (Figure S1A; [20]). The boundary density reaches a maximum of ∼22% total sites at ∼50% filament occupancy.

more flexible than native filaments (Figure S2A and [18, 19]). It is hypothesized that shear stress associated with thermal-induced fluctuations accumulates locally at boundaries of mechanical asymmetry, thereby leading to preferential severing at junctions of bare and decorated filament segments [3, 12, 14, 19, 20].

To test the prediction of preferential severing at boundaries of bare and decorated segments, we quantified the severing events occurring during spontaneous assembly of ATP-actin filaments. Line scans of fluorescence intensity along actin filaments reveal that fragmentation is statistically favored at sites of low ADF/cofilin binding density and occurs exclusively outside the ATP/ADP-P_i cap (Figures 4A–4C). Note that severing is not obligatory with ADF/cofilin binding, but the frequency of severing events correlates with the position (Figures 4A and 4B) and density (Figure 4D) of bare and ADF/cofilin-decorated boundaries, consistent with preferential severing at or near these boundaries on filaments (Movie S4).

Concluding Remarks
ADF/Cofilin Modulates the Nucleotide Composition of Growing Actin Filaments
The age and stability of actin filaments is linked to the chemical state of the bound adenine nucleotide. ATP bound to monomers is rapidly hydrolyzed after incorporation into filaments such that freshly polymerized filaments are comprised of subunits with bound ATP or ADP-P_i, whereas older filament subunits release P_i slowly and have bound ADP. The actin-binding activities of many actin-binding proteins (ABPs) including ADF/cofilin are sensitive to the chemical state of the actin-bound nucleotide, so the filament nucleotide composition dramatically influences the organization, stability, and dynamics of cellular actin-based structures.

ADF/cofilin ages filaments by accelerating P_i release over an order of magnitude. This effect is allosteric and propagates to distal sites unoccupied by ADF/cofilin, presumably through allosteric modulation of filament twist and dynamics [13, 21, 22]. Therefore, a kinetic competition between monomer addition, intrinsic random ATP hydrolysis [23] and P_i release [5], ADF/cofilin binding [5, 11, 12], and allosteric ADF/cofilin-mediated acceleration of P_i release (Figure 3B) exists during assembly and network growth.

P_i release, though accelerated allosterically by ADF/cofilin, remains considerably slower than filament elongation (up to 500 subunits s^{-1}) at high in vivo actin concentrations, which yields a large filament ATP/ADP-P_i cap (∼100 μm in length) that precludes ADF/cofilin binding and severing. Even if the P_i release is faster for yeast actin [24], this behavior is difficult to reconcile with the observation that ADF/cofilin binds growing cellular filaments only 0.2–1 μm away from their nucleation sites [25–27]. We favor a mechanism in which filament barbed ends must be rapidly capped (to stop rapid elongation) for significant ADF/cofilin binding to occur. Such a mechanism

would account for colocalization of ADF/cofilin and capping protein in actin networks [26] and modulation of ADF/cofilin severing efficiency by capping protein. Subsequent ADF/cofilin binding to stochastically emerging ADP subunits of capped filaments allosterically accelerates P_i release, thereby promoting Arp2/3 complex dissociation [10] and network remodeling. Therefore, although ADF/cofilin-mediated acceleration of P_i release minimally affects the ATP/ADP-P_i cap length of rapidly elongating filaments in vivo, it rapidly ages filaments and networks by allosterically accelerating P_i release once they are capped and stop elongating.

ADF/Cofilin Preferentially Severs ADP-Actin Filaments at Boundaries of Bare and Cofilin-Decorated Segments

Quantitative analysis of filament binding [5, 9, 11, 12, 20, 28] and severing [3, 29, 30] indicates that ADF/cofilin severing activity scales with the density of boundaries between bare and ADF/cofilin-decorated filament segments [14]. It has been hypothesized that asymmetry originating from discontinuities in filament topology and mechanics (i.e., bending and twisting elasticity) generates a local accumulation of shear stress [19], thereby leading to preferential fragmentation at or near these boundaries [14]. This hypothesis relies on three important observations: (1) severing occurs at low ADF/cofilin binding densities and small cluster sizes [20, 29, 30]; (2) cofilin-decorated filaments display significantly different mechanical properties from bare filaments [13, 18, 19]; (3) partially ADF/cofilin-decorated filaments are considerably less stable than bare or ADF/cofilin-saturated filaments [21, 22].

The prediction that ADF/cofilin-mediated severing occurs at bare and decorated boundaries lacks direct proof and is best evaluated by direct, real-time visualization of ADF/cofilin binding and filament severing, as performed in this study. Severing is not obligatory with ADF/cofilin binding, but the frequency of severing events scales with the boundary density and also occurs at or near these boundaries. These observations lend credence to the hypothesis that shear stress accumulates at a mechanical asymmetry presented at boundaries of bare and ADF/cofilin-decorated filament segments, thereby promoting severing. A challenge for future investigations will be to determine how other actin-binding proteins, including coronin and AiP1 [31], modulate this mechanism to promote actin disassembly.

Supplemental Information

Acknowledgments

References

1. Pollard, T.D., Blanchoin, L., and Mullins, R.D. (2000). Molecular mechanisms controlling actin filament dynamics in nonmuscle cells. Annu. Rev. Biophys. Biomol. Struct. *29*, 545–576.

2. Loisel, T.P., Boujemaa, R., Pantaloni, D., and Carlier, M.F. (1999). Reconstitution of actin-based motility of Listeria and Shigella using pure proteins. Nature *401*, 613–616.

3. Michelot, A., Berro, J., Guérin, C., Boujemaa-Paterski, R., Staiger, C.J., Martiel, J.L., and Blanchoin, L. (2007). Actin-filament stochastic dynamics mediated by ADF/cofilin. Curr. Biol. *17*, 825–833.

4. Lappalainen, P., Fedorov, E.V., Fedorov, A.A., Almo, S.C., and Drubin, D.G. (1997). Essential functions and actin-binding surfaces of yeast cofilin revealed by systematic mutagenesis. EMBO J. *16*, 5520–5530.

5. Blanchoin, L., and Pollard, T.D. (1999). Mechanism of interaction of *Acanthamoeba* actophorin (ADF/Cofilin) with actin filaments. J. Biol. Chem. *274*, 15538–15546.

6. Achard, V., Martiel, J.L., Michelot, A., Guérin, C., Reymann, A.C., Blanchoin, L., and Boujemaa-Paterski, R.A. (2010). A "primer"-based mechanism underlies branched actin filament network formation and motility. Curr. Biol. *20*, 423–428.

7. Bobkov, A.A., Muhlrad, A., Kokabi, K., Vorobiev, S., Almo, S.C., and Reisler, E. (2002). Structural effects of cofilin on longitudinal contacts in F-actin. J. Mol. Biol. *323*, 739–750.

8. Vavylonis, D., Yang, Q., and O'Shaughnessy, B. (2005). Actin polymerization kinetics, cap structure, and fluctuations. Proc. Natl. Acad. Sci. USA *102*, 8543–8548.

9. Roland, J., Berro, J., Michelot, A., Blanchoin, L., and Martiel, J.L. (2008). Stochastic severing of actin filaments by actin depolymerizing factor/cofilin controls the emergence of a steady dynamical regime. Biophys. J. *94*, 2082–2094.

10. Chan, C., Beltzner, C.C., and Pollard, T.D. (2009). Cofilin dissociates Arp2/3 complex and branches from actin filaments. Curr. Biol. *19*, 537–545.

11. Cao, W., Goodarzi, J.P., and De La Cruz, E.M. (2006). Energetics and kinetics of cooperative cofilin-actin filament interactions. J. Mol. Biol. *361*, 257–267.

12. De La Cruz, E.M., and Sept, D. (2010). The kinetics of cooperative cofilin binding reveals two states of the cofilin-actin filament. Biophys. J. *98*, 1893–1901.

13. Prochniewicz, E., Janson, N., Thomas, D.D., and De la Cruz, E.M. (2005). Cofilin increases the torsional flexibility and dynamics of actin filaments. J. Mol. Biol. *353*, 990–1000.

14. De La Cruz, E.M. (2009). How cofilin severs an actin filament. Biophys. Rev. *1*, 51–59.

15. McGough, A., Pope, B., Chiu, W., and Weeds, A. (1997). Cofilin changes the twist of F-actin: Implications for actin filament dynamics and cellular function. J. Cell Biol. *138*, 771–781.

16. Galkin, V.E., Orlova, A., Lukoyanova, N., Wriggers, W., and Egelman, E.H. (2001). Actin depolymerizing factor stabilizes an existing state of F-actin and can change the tilt of F-actin subunits. J. Cell Biol. *153*, 75–86.

17. Muhlrad, A., Kudryashov, D., Michael Peyser, Y., Bobkov, A.A., Almo, S.C., and Reisler, E. (2004). Cofilin induced conformational changes in F-actin expose subdomain 2 to proteolysis. J. Mol. Biol. *342*, 1559–1567.

18. Pfaendtner, J., De La Cruz, E.M., and Voth, G.A. (2010). Actin filament remodeling by actin depolymerization factor/cofilin. Proc. Natl. Acad. Sci. USA *107*, 7299–7304.

19. McCullough, B.R., Blanchoin, L., Martiel, J.L., and De la Cruz, E.M. (2008). Cofilin increases the bending flexibility of actin filaments: Implications for severing and cell mechanics. J. Mol. Biol. *381*, 550–558.

20. De La Cruz, E.M. (2005). Cofilin binding to muscle and non-muscle actin filaments: Isoform-dependent cooperative interactions. J. Mol. Biol. *346*, 557–564.

21. Bobkov, A.A., Muhlrad, A., Pavlov, D.A., Kokabi, K., Yilmaz, A., and Reisler, E. (2006). Cooperative effects of cofilin (ADF) on actin structure suggest allosteric mechanism of cofilin function. J. Mol. Biol. *356*, 325–334.

22. Dedova, I.V., Nikolaeva, O.P., Safer, D., De La Cruz, E.M., and dos Remedios, C.G. (2006). Thymosin beta4 induces a conformational change in actin monomers. Biophys. J. *90*, 985–992.

23. Blanchoin, L., and Pollard, T.D. (2002). Hydrolysis of ATP by polymerized actin depends on the bound divalent cation but not profilin. Biochemistry *41*, 597–602.

24. Ti, S.C., and Pollard, T.D. (2011). Purification of actin from fission yeast Schizosaccharomyces pombe and characterization of functional differences from muscle actin. J. Biol. Chem. *286*, 5784–5792.

25. Svitkina, T.M., and Borisy, G.G. (1999). Arp2/3 complex and actin depolymerizing factor/cofilin in dendritic organization and treadmilling of actin filament array in lamellipodia. J. Cell Biol. *145*, 1009–1026.

26. Iwasa, J.H., and Mullins, R.D. (2007). Spatial and temporal relationships between actin-filament nucleation, capping, and disassembly. Curr. Biol. *17*, 395–406.

27. Okreglak, V., and Drubin, D.G. (2007). Cofilin recruitment and function during actin-mediated endocytosis dictated by actin nucleotide state. J. Cell Biol. *178*, 1251–1264.

28. Ressad, F., Didry, D., Xia, G.X., Hong, Y., Chua, N.H., Pantaloni, D., and Carlier, M.F. (1998). Kinetic analysis of the interaction of actin-depolymerizing factor (ADF)/cofilin with G- and F-actins. Comparison of plant and human ADFs and effect of phosphorylation. J. Biol. Chem. *273*, 20894–20902.

29. Andrianantoandro, E., and Pollard, T.D. (2006). Mechanism of actin filament turnover by severing and nucleation at different concentrations of ADF/cofilin. Mol. Cell *24*, 13–23.

30. Pavlov, D., Muhlrad, A., Cooper, J., Wear, M., and Reisler, E. (2007). Actin filament severing by cofilin. J. Mol. Biol. *365*, 1350–1358.

31. Kueh, H.Y., Charras, G.T., Mitchison, T.J., and Brieher, W.M. (2008). Actin disassembly by cofilin, coronin, and Aip1 occurs in bursts and is inhibited by barbed-end cappers. J. Cell Biol. *182*, 341–353.